Relationship between Orbital Optic Nerve Axon Counts and Retinal Nerve Fiber Layer Thickness Measured by Spectral Domain Optical Coherence Tomography

Grant A. Cull, Juan Reynaud, Lin Wang, George A. Cioffi, Claude F. Burgoyne, and Brad Fortune

Purpose. We determined the relationship between total optic nerve axon counts and peripapillary retinal nerve fiber layer thickness (RNFLT) measured in vivo by spectral domain optical coherence tomography (SDOCT).

Methods. A total of 22 rhesus macaques had three or more baseline measurements in both eyes of peripapillary RNFLT made by SDOCT. Laser photocoagulation then was applied to the trabecular meshwork of one eye to induce chronic unilateral IOP elevation. SDOCT measurements of RNFLT continued approximately every two weeks until the predefined study endpoint was reached in each animal. At endpoint, animals were sacrificed and the optic nerve was sampled approximately 2 mm behind the globe to obtain thin sections for histologic processing and automated axon counting across 100% of the optic nerve cross-sectional area.

Results. At the final imaging session, the average loss of RNFLT was 20 ± 21%, ranging from essentially no loss to nearly 65% loss. Total optic nerve axon count in control eyes ranged from 812,478 to 1,280,474. The absolute number of optic nerve axons was related linearly to RNFLT (axon count = 12,336 × $RNFLT_{(\mu m)}$ − 257,050, $R^2 = 0.65$, $P < 0.0001$), with a Pearson correlation coefficient of 0.81. There also was a strong linear relationship between relative optic nerve axon loss (glaucomatous-to-control eye) and relative RNFLT at the final imaging session, with a slope close to unity but a significantly negative intercept (relative axon $loss_{(\%)} = 1.05 \times$ relative RNFLT $loss_{(\%)} -$ 14.4%, $R^2 = 0.75$, $P < 0.0001$). The negative intercept was robust to variations of fitted model because relative axon loss was −14% on average for all experimental glaucoma (EG) eyes within 6% (measurement noise) of zero relative loss.

Conclusions. There is a strong linear relationship between total optic nerve axon count and RNFLT measured in vivo by SDOCT. However, substantial loss of optic nerve axons (~10%–15%) exists before any loss of RNFLT manifests and this discrepancy persists systematically throughout a wide range of damage. (*Invest Ophthalmol Vis Sci.* 2012;53:7766–7773) DOI: 10.1167/iovs.12-10752

From the Discoveries in Sight Research Laboratories, Devers Eye Institute, and Legacy Research Institute, Legacy Health, Portland, Oregon.

Supported by Grants NIH R01-EY019327 (BF), R01-EY011610 (CFB), and R01-EY019939 (LW); Legacy Good Samaritan Foundation; and Heidelberg Engineering, GmbH, Heidelberg, Germany (equipment).

Submitted for publication August 10, 2012; revised September 26, 2012; accepted October 22, 2012.

Disclosure: **G.A. Cull**, None; **J. Reynaud**, None; **L. Wang**, None; **G.A. Cioffi**, None; **C.F. Burgoyne**, Heidelberg Engineering (F); **B. Fortune**, Heidelberg Engineering (F)

Corresponding author: Brad Fortune, Devers Eye Institute, 1225 NE Second Avenue, Portland, OR 97232; bfortune@deverseye.org.

Clinical measurement of retinal nerve fiber layer thickness (RNFLT), by spectral domain optical coherence tomography (SDOCT) for example, has become an important tool for diagnosis and management of glaucoma and other optic neuropathies.[1,2] Measurements of RNFLT can be obtained rapidly in a clinical setting, and are known to have excellent reproducibility and diagnostic accuracy.[1,2] OCT measurements of RNFLT also have been shown to agree with histomorphometric measurements of RNFLT obtained from nonhuman primates with experimental glaucoma.[3]

An underlying premise of clinical RNFLT measurements is that they represent an estimate of the number of retinal ganglion cell axons entering the optic nerve, an anatomic quantity that can be obtained otherwise only postmortem by histologic methods. If this premise proves to be true, such measurements would represent a meaningful anatomic parameter that clinicians could use to monitor the stability of individual patients and to assess efficacy of therapeutic interventions. Moreover, such a parameter eventually might serve as a potential outcome measure or endpoint for future clinical trials of novel therapeutics.[4] There also is growing interest in understanding the relationship between RNFLT and measures of vision function, such as perimetric sensitivity,[5–7] given that at some fundamental level each retinal ganglion cell conveys a continuous important functional message to the brain.[8] Thus, it is important to understand how measurements of the RNFLT made in vivo, such as those by SDOCT, relate to the number of retinal ganglion cell axons within the optic nerve.

Reynaud et al. recently reported the details and validation of a novel automated method for counting 100% of the axons present within an optic nerve cross-section.[9] Counting 100% of the optic nerve cross-sectional area instead of sampling smaller, representative areas reduces estimation error, thus increasing the accuracy of the total count.[9,10] With the benefit of this newly developed technique, our study was designed to evaluate the relationship between RNFLT measured by SDOCT, and the total number of optic nerve axons in control and glaucomatous eyes of nonhuman primates with unilateral experimental glaucoma.

Methods

Subjects

The primary subjects of our study were 22 rhesus macaque monkeys (*Macaca mulatta*) with unilateral experimental glaucoma. Table 1 lists the age, weight, and sex of each animal. An additional five monkeys (three male, two female) were included as bilateral controls for optic nerve axon counts. Both eyes of each of these five animals were normal. Their ages were 2, 8, 8, 9, and 9 years. They were not included in any other aspect of the study. All experimental methods and animal care procedures adhered to the Association for Research in Vision and Ophthalmology's Statement for the Use of Animals in Ophthalmic and

Investigative Ophthalmology & Visual Science, November 2012, Vol. 53, No. 12

Table 1. Study Subjects Age, Weight, Sex, and IOP Information

Animal ID	Age, y	Sex	Wt., kg	Duration First Laser to Sacrifice, mo	Mean IOP, mm Hg		Peak IOP, mm Hg		Cumulative IOP Difference, mm Hg × Days
					Control	EG	Control	EG	
AM89	21.9	M	8.9	4.7	13.3	16.2	19.7	42.0	343.7
26161	1.4	F	3.3	7.4	8.4	11.7	14.3	37.0	564.2
22159	19.7	F	8.2	13.9	9.9	14.2	15.0	23.0	1,881.7
AM76	21.9	F	8.6	9.0	11.3	16.5	19.0	38.0	1,228.8
137	9.6	M	13.0	8.2	16.4	30.5	22.3	49.0	3,725.4
AO23	20.0	F	7.2	5.8	10.4	17.7	15.0	38.0	1,233.7
18664	15.1	F	5.9	4.9	8.7	10.4	12.3	15.3	251.5
26072	1.5	F	4.1	8.2	8.5	10.9	15.3	32.3	457.6
23499	9.9	F	4.9	7.4	11.0	14.7	15.3	45.7	803.3
25564	2.3	F	3.7	6.0	9.0	12.4	16.0	28.0	591.3
AP02	18.6	F	5.6	5.2	9.3	15.4	13.3	41.0	756.3
25357	2.6	M	5.5	8.1	9.0	12.0	13.3	28.7	689.7
25356	4.1	M	5.1	6.1	8.4	20.8	13.3	44.7	2,291.7
136	10.6	M	13.9	12.8	13.5	29.6	19.0	51.5	6,807.9
21676	12.5	F	5.4	8.4	10.5	14.8	18.0	42.7	949.7
140	8.8	F	6.1	8.3	8.9	11.1	16.0	35.7	498.3
23538	10.7	F	4.9	6.8	11.1	17.8	19.0	42.7	1,324.3
139	9.1	F	6.2	12.0	12.7	21.1	19.3	52.7	3,679.7
15527	21.1	F	8.5	3.3	12.6	31.0	17.7	54.0	1,777.7
25904	1.2	F	6.4	4.1	11.5	31.9	16.0	43.0	2,338.3
135	10.6	M	11.4	12.6	10.7	14.1	18.7	40.3	1,404.0
20377	9.2	F	5.9	19.7	11.6	29.3	19.0	57.3	10,727.0
Average	11.0	16 F	6.9	8.3	10.8	18.4	16.7	40.1	2,014.8
SD	7.1	6 M	2.8	3.9	2.1	7.3	2.6	10.3	2,465.1

Wt., weight.

Vision Research, and were approved and monitored by the Institutional Animal Care and Use Committee at Legacy Health.

Anesthesia

All experimental procedures began with induction of general anesthesia using ketamine (15 mg/kg IM) in combination with either xylazine (0.8–1.5 mg/kg IM) or midazolam (0.2 mg/kg IM), along with a single subcutaneous injection of atropine sulfate (0.05 mg/kg). Laser photocoagulation of the trabecular meshwork (to induce chronic elevation of IOP) was performed under this induction dose. To maintain anesthesia during SDOCT imaging sessions, animals were intubated after induction and breathed 100% oxygen mixed with isoflurane gas (1%–2%, typically 1.25%). Intravenous fluids (lactated Ringer's solution, 10 mL/kg/h) were administered via the saphenous vein during imaging sessions. Vital signs were monitored throughout all imaging sessions including, heart rate, blood pressure, arterial oxyhemoglobin saturation, end-tidal CO_2, and body temperature. Body temperature was maintained at 37° C, heart rate above 75 per minute, and oxygen saturation above 95%.

SDOCT Imaging Sessions: Peripapillary RNFL Thickness

To begin each imaging session, the animal was placed in the prone position, topical corneal anesthetic (0.5% proparacaine) was applied to each eye, a lid speculum was inserted, and IOP was measured using an applanation tonometer (Tonopen XL; Reichert Technologies, Inc., Depew, NY). The value recorded for each eye was the average of three successive measurements. Pupillary dilation was induced (0.5% tropicamide and 2.5% phenylephrine) and a clear, plano-powered, rigid gas-permeable contact lens was placed on each eye with topical lubricant (0.5% carboxymethylcellulose sodium, Refresh; Allergan, Irvine, CA). All SDOCT scans were performed 30 minutes after IOP was lowered manometrically to 10 mm Hg.

Peripapillary RNFLT was measured using a commercial SDOCT instrument (Spectralis; Heidelberg Engineering GmbH, Heidelberg, Germany). For our study, the average peripapillary RNFLT was measured from a single circular B-scan consisting of 1536 A-scans. Nine to 16 individual sweeps were averaged in real time to comprise the final stored B-scan at each session. At the initial imaging session, the operator centered the position of the scan on the optic nerve head (ONH, based on the view of the optic disc margin in the corresponding infrared reflectance image) and all subsequent scans were pinned (identical) to this location. A trained technician manually corrected the accuracy of the instrument's native automated layer segmentations when the algorithm obviously had erred from the inner and outer borders of the RNFL to an adjacent layer (such as a refractive element in the vitreous instead of the internal limiting membrane, or to the inner plexiform layer instead of the outer border of the RNFL). All segmentations then were exported for extraction of RNFLT values by custom software. All SDOCT scans in our study had an acceptable quality score above 15 (99% were $\geq$20, the average $\pm$ SD was 30.1 $\pm$ 4.3), and there were no differences between control eyes and glaucomatous eyes ($P = 0.46$, paired *t*-test).

Experimental Glaucoma

Each animal had a minimum of three (average of 5) weekly baseline SDOCT recordings before induction of unilateral experimental glaucoma (EG). Then, argon laser photocoagulation was applied to the trabecular meshwork of one eye of each animal to induce chronic elevation of IOP. Initially, 180° of the trabecular meshwork was treated in one session. The remaining 180° was treated in a second session approximately two weeks later. If necessary, laser treatments were repeated in subsequent weeks (limited to a 90° sector) until an IOP elevation was noted first or if the initial post-laser IOP had returned to

Table 2. RNFLT (μm) at Baseline (BL ave) and Final Imaging Session, and Optic Nerve Axon Count for Each Eye

	RNFLT						
	BL Ave		Final		Optic Nerve Axon Count		Relative Optic Nerve Axon Count
Animal ID	Control	EG	Control	EG	Control	EG	(EG:Control)
AM89	98.9	101.7	100.3	101.6	812,478	820,768	1.01
26161	107.0	100.8	104.2	83.6	924,615	882,865	0.95
22159	91.9	95.4	94.1	97.6	1,123,945	1,046,638	0.93
AM76	96.6	96.0	97.4	92.7	1,237,367	1,087,556	0.88
137	99.1	97.9	99.5	94.1	1,013,864	885,910	0.87
AO23	87.7	84.9	87.1	84.3	1,112,954	964,987	0.87
18664	108.2	109.8	105.0	88.8	1,114,604	959,358	0.86
26072	95.0	93.4	96.4	101.6	1,030,622	874,974	0.85
23499	93.4	95.5	90.3	89.4	867,124	730,665	0.84
25564	92.3	94.7	89.2	89.4	1,045,003	866,195	0.83
AP02	93.1	92.2	89.5	86.7	1,024,432	785,288	0.77
25357	100.4	98.6	99.6	93.8	964,903	689,934	0.72
25356	116.0	113.8	119.4	96.1	1,270,010	633,876	0.50
136	135.0	142.2	129.3	86.4	1,280,474	621,047	0.49
21676	91.3	87.3	90.3	63.2	1,073,047	478,677	0.45
140	105.7	102.5	109.0	64.4	856,757	379,697	0.44
23538	98.1	98.9	97.8	82.3	980,175	415,375	0.42
139	104.8	105.0	103.4	61.8	952,704	389,396	0.41
15527	96.4	96.8	101.7	37.2	1,218,141	389,235	0.32
25904	99.7	99.5	100.5	36.0	1,085,661	300,788	0.28
135	98.4	98.9	102.6	62.8	896,426	235,087	0.26
20377	103.4	102.9	105.4	57.5	999,654	259,499	0.26
Average	100.6	100.4	100.5	79.6	1,040,225	668,083	0.65
SD	10.1	11.3	9.9	19.3	132,951	270,834	0.26

normal levels. The average number of laser treatments (± SD) was 6.0 ± 3.0.

Imaging by SDOCT was repeated during the post-laser follow-up period approximately every two weeks until the predefined study endpoint had been reached for each animal. Specific endpoints were based on the primary study to which each animal was assigned and were determined based on those specific protocols. Thus, the specific endpoint targets and details of sacrifice procedures differed across animals and in most cases did not include any specific outcome for RNFLT (rather, e.g., onset of change in ONH surface topography measured by HRT or onset of functional changes measured by electroretinography). Some animals were sacrificed at an "early" stage, while others were followed to later stages of glaucomatous damage. The varied endpoints across the group enabled a range of severity to be evaluated in our study.

Retrobulbar Axon Counts

Animals were sacrificed under deep anesthesia (either pentobarbital IV or isoflurane inhalation) and tissues were preserved in most cases by perfusion fixation with either 4% paraformaldehyde or 4% paraformaldehyde followed by 5% glutaraldehyde; in 6 of the 22 animals, the eyes were immersion fixed in 4% paraformaldehyde immediately after enucleation.

A 2 to 3 mm sample of each optic nerve, beginning 2 mm posterior to the globe, was cut with a Vibratome (VT 100S; Leica Microsystems GmbH, Wetzlar, Germany) into 0.5 mm thick transverse sections. Each of these thick optic nerve sections was post-fixed in 4% osmium tetroxide and embedded in epoxy resin. Optic nerve cross-sections (1 μm thick) then were cut and stained with p-phenylenediamine and mounted on glass slides. The most complete and uniformly stained section from each optic nerve then was chosen for axon counting.

Axon counts for 100% of the optic nerve cross-sectional area were obtained by methods validated and described in detail recently.[9] Images covering 100% of the optic nerve cross-section were captured automatically using an inverted light microscope (DM IRB; Leica Microsystems GmbH) with an oil immersion 100× objective (PL Fluotar NA = 1.3; Leica Microsystems GmbH), imaging software (Bioquant Imaging System, NOVA; R&M Biometrics, Inc., Nashville, TN), and a computer controlled X-Y-Z stage (Applied Scientific Instrumentation, Inc., Eugene, OR). Each acquired image was 640 × 480 pixels (width × height) covering an area of 1412 μm². Each image was saved in Bioquant's BIF format, which contains the image's x,y coordinates relative to a user-selected center. Automated axon counting software[9] was used to count all of the axons with normal morphologic characteristics in each optic nerve cross-section. The total axon count for each optic nerve was represented by the sum of all counted axons across all images tiling its entire cross-sectional area.

Results

Animals were followed for an average of 8.3 months after the first laser application to the EG eye (range 3.3–19.7 months, Table 1). Over the duration of follow-up, mean IOP in the EG eyes was 6 mm Hg higher, on average, than that in fellow control eyes. Peak IOP was 40 mm Hg on average in EG eyes and never was observed to be above 60 mm Hg.

Table 2 lists the values of RNFLT at baseline and at the final imaging session, as well as the axon count for each eye. The list is ordered by increasing degree of glaucomatous axon loss in the EG eyes (i.e., by axon count in the EG eye relative to the control eye). Note that the baseline value of RNFLT represents the average of all baseline observations for each eye. Among the 22 fellow control eyes, the total optic nerve axon count ranged from 812,478 to 1,280,474. This range was similar to the total axon count observed in the group of 10 eyes from the five bilateral control animals (785,532–1,213,954). There was no significant effect of age on total axon count in the group of 22 fellow control eyes (axon count = $3722 \times \text{age}_{(\text{yrs})} + 994{,}141$,

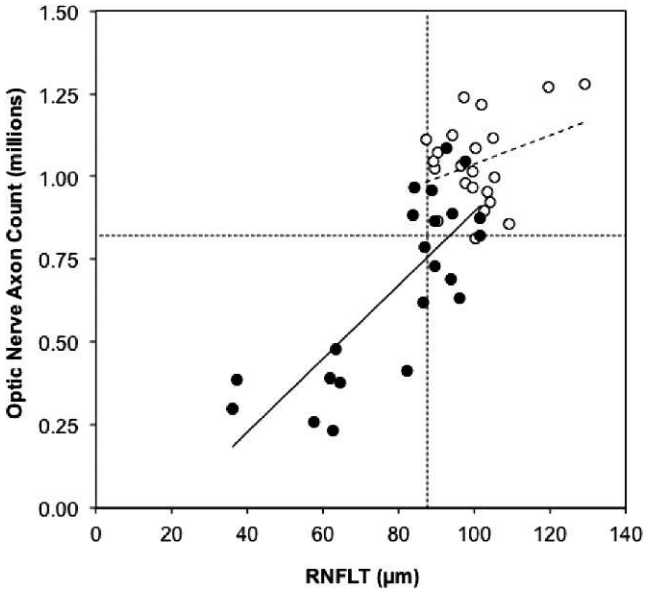

Figure 1. Absolute count of optic nerve axons versus RNFLT at the final time point. Control eyes are represented by *open symbols*, EG eyes by *filled symbols*. The *dotted horizontal* and *vertical lines* represent the lower limit of the control eye distribution (first percentile) of optic nerve axon counts and RNFLT, respectively. The *dashed* and *solid lines* represent the results of linear regression for control and EG eyes, respectively.

$R^2 = 0.04$, $P = 0.39$). Including the additional five bilateral control animals (using the average axon count from each of these pairs of eyes) did not alter this relationship (axon count = $3535 \times \text{age}_{(\text{yrs})} + 1{,}000{,}926$, $R^2 = 0.03$, $P = 0.39$).

Figure 1 shows that the absolute number of optic nerve axons can be predicted reasonably accurately from the absolute values of RNFLT (axon count = $12{,}336 \times \text{RNFLT}_{(\mu\text{m})} - 257{,}050$, $R^2 = 0.65$, $P < 0.0001$). However, there is a significant difference between the relationships when the EG and control eyes are considered separately ($F = 8.8$, $P = 0.005$). The relationship between total optic nerve axon count and RNFLT in the control eyes is not particularly strong (axon count = $4324 \times \text{RNFLT}_{(\mu\text{m})} + 605{,}424$, $R^2 = 0.10$, $P = 0.15$). In contrast, this relationship has a stronger association among the group of EG eyes (axon count = $11{,}083 \times \text{RNFLT}_{(\mu\text{m})} - 214{,}208$, $R^2 = 0.63$, $P < 0.0001$), which appears to be driving the results for all eyes considered together. Figure 1 also shows that there is substantial overlap between the EG and control eye values for both measures, with 9 of 22 EG eyes having one or both values within the normal range (first percentile of control eye values). This underscores the difficulty of achieving high diagnostic sensitivity on the basis of cross-sectional comparisons.

RNFLT should be linearly proportional to the number of axons within the RNFL, at least for longitudinal change assuming that the RNFL "collapses" to a compact bundle packing as axons are lost (this assumption is well supported by published[11] and other unpublished observations). A linear model also is simplest and, thus, was our a priori choice. However, there is a well known "floor effect" for RNFLT[12–14] whereby complete loss of all axons results in a plateau value of approximately 30% to 40% of the average normal RNFLT. The range of severity in our study did not include that end-stage level of damage; the two animals with the most severe damage each had 74% loss of optic nerve axons (Table 2). Nevertheless, it was prudent to evaluate alternative models to fit these data. The fitness of exponential and higher-order polynomial models was compared to the linear model for each data set (all eyes combined, and the EG and control eye groups fit separately) using *F*-tests and Akaike's Information Criterion (AIC) differences. In all cases, the linear model was most appropriate. Second-order polynomial (quadratic) models produced marginally better fits (slightly higher R^2 values, as expected, given their greater number of degrees of freedom); however, the fits never were statistically significantly better than that provided by the linear model (e.g., linear versus quadratic fit, $F_{[1,41\text{df}]} = 0.005$, $P = 0.95$, and AIC difference = −4.5 for all eyes combined, and $F_{[1,19\text{df}]} = 1.6$, $P = 0.22$, and AIC difference = −1.3 for EG eyes alone), indicating the linear model was superior. The appropriateness of the linear model also was confirmed in each case by performing a runs test and normality test (D'Agostino-Pearson omnibus K2) on the residuals. Finally, it should be noted that in every case the best fit of either the exponential or quadratic model produced results opposite to what would have been predicted if the floor effect for RNFLT had been operative: the slight bend in the best-fit function always was oriented toward the lower right of the graph not the upper left, though this is moot since the linear fits were statistically superior in each case.

One advantage of inducible glaucoma models is the ability to limit the experimental injury to just one eye, while the fellow eye serves as an internal control. This type of study design capitalizes on the tendency toward interocular symmetry, which often can help overcome a degree of population variance, such as was evident in Figure 1. The following analysis was performed to determine whether interocular estimates of glaucomatous RNFL loss could serve as an accurate predictor of longitudinal within-eye measures of loss, since the optic nerve axon count data are limited naturally to just cross-sectional (interocular) estimates.

To begin, there was no significant difference at baseline between fellow eye pairs for RNFLT ($P = 0.77$, paired *t*-test). The average RNFLT difference between fellow eyes at baseline was 2.1 ± 1.7% and 95% of fellow eye pairs were within a 5% difference. Baseline values of RNFLT in the EG eye group are plotted against control eye values in Figure 2, demonstrating a strong linear relationship ($R^2 = 0.94$). Thus, baseline values of RNFLT in one eye are highly predictive of values in the fellow eye.

At the final imaging session, the average loss of RNFLT was 20 ± 21%, ranging from essentially no loss to nearly 65% loss (Table 2). RNFLT loss in the EG eyes can be expressed in two ways: relative to the baseline value within the same eye (longitudinal estimate) or relative to the fellow control eye value at the same final imaging session (cross-sectional estimate). Figure 3 demonstrates that the cross-sectional estimate of loss is highly predictive of the longitudinal estimate of loss ($y = 0.97x - 0.007$, $R^2 = 0.98$). This is important because it enables optic nerve axon loss estimates, which are limited to the cross-sectional method (EG:control eye), to be compared reasonably with RNFLT loss using the same method.

Relative optic nerve axon loss is plotted in Figure 4 versus relative RFNLT loss at the final imaging session. Again the best model to fit these data was evaluated using *F*-tests and AIC differences. The slightly better fit of the quadratic model ($R^2 = 0.77$) over a linear model ($R^2 = 0.75$) was not sufficient to risk over-fitting (i.e., to reject the null hypothesis that the linear model was superior; $F_{[1,19\text{df}]} = 1.7$, $P = 0.21$, AIC difference = −1.2). Similarly, a linear model was superior to an exponential function (AIC difference = −7.3). Therefore a linear model was adopted for this analysis. The results of linear regression reveal two important findings: there is a reasonably strong linear relationship with a slope close to unity, but an intercept with an unequivocally negative value (relative axon $\text{loss}_{(\%)} = 1.05 \times$

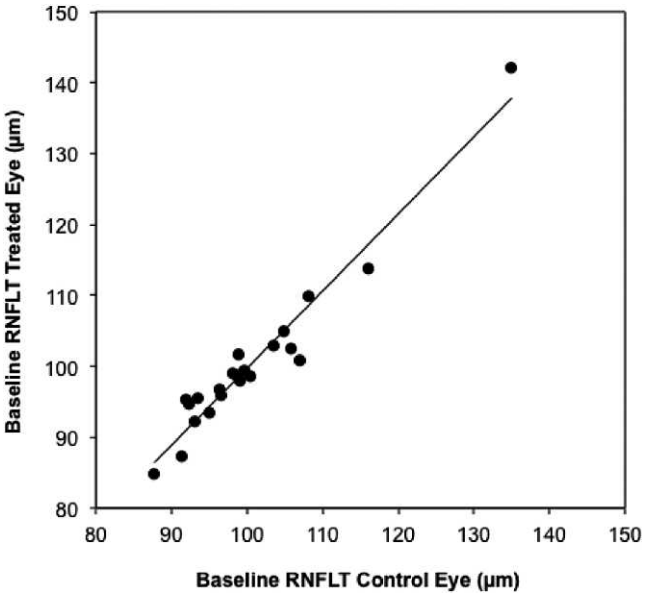

Figure 2. Baseline values of RNFLT for EG eyes plotted versus control eye values; *line* represents results of linear regression ($y = 1.09x$ – 8.9, $R^2 = 0.94$).

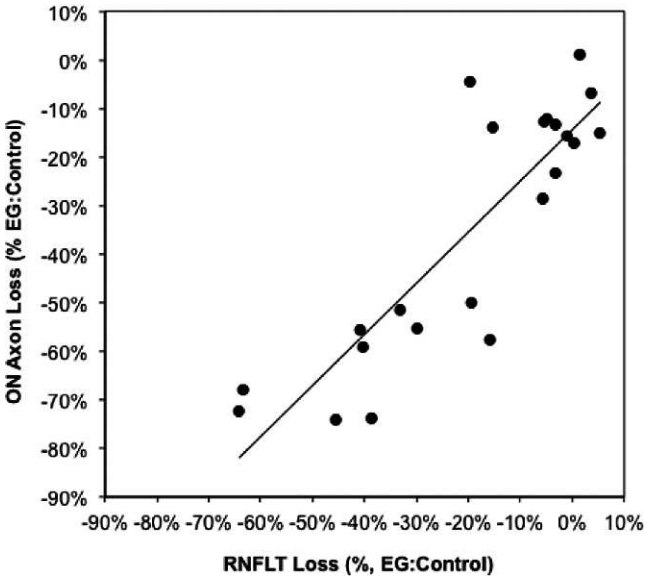

Figure 4. Optic nerve axon loss versus RNFLT loss in the EG eyes at the final imaging session. The *line* represents results of linear regression ($y = 1.05x - 14.4$, $R^2 = 0.75$).

relative RNFLT $\text{loss}_{(\%)} - 14.4\%$, $R^2 = 0.75$, $P < 0.0001$). The 95% confidence interval (CI) for the intercept was –6.3% to –22.5%. This did not overlap with the range of interocular differences observed among the five pairs of bilateral control eyes, which centered close to zero; the mean difference between pairs of bilateral control eyes (± SD) was 0.6% (± 1.7%); the 95% CI ranged from –1.2% to +2.8%. Note also that the best fit quadratic model produced an intercept term of –12.2% axon loss at zero RNFLT loss. This primarily is because the average axon loss among the EG eyes within 6% (measurement noise) of zero relative RNFLT loss was 14.2% (see data around the origin of Fig. 4 and in Table 2).

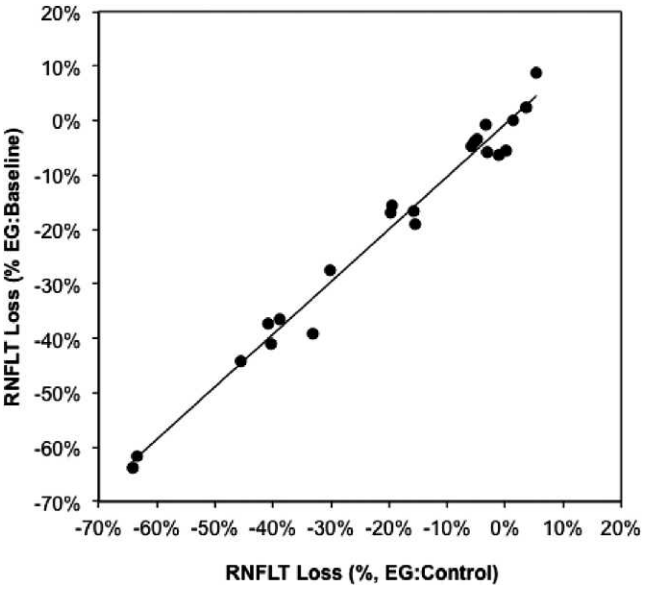

Figure 3. RNFLT loss in the EG eyes at the final imaging session. RNFLT loss in the EG eyes is calculated in two ways: the value at the final session relative to the baseline value within the same eyes (*longitudinal*, *ordinate*) and the value at the final session relative to the fellow control eye value at the same final imaging session (*cross-sectional*, *abscissa*). The *line* represents results of linear regression ($y = 0.97x - 0.007$, $R^2 = 0.98$).

There are two clear implications of this finding. First, RNFLT measured in vivo by SDOCT can provide a reasonably accurate estimate of optic nerve axon loss over a wide range of experimental disease severity. Second, the estimate based on RNFLT is approximately 14.4% less than the actual axon loss within the retrobulbar optic nerve even at the earliest stage of detectable RNFLT loss, and the magnitude of this underestimate increases slightly as the disease progresses. Thus, the results from this cohort of 22 nonhuman primates with EG provide clear evidence that optic nerve axon loss already is substantial before RNFLT loss manifests and that this discrepancy persists over a wide range of severity that approached 75% axon loss in our study.

Ordinary least squares linear regression was used because the primary purpose of this analysis was to determine if RNFLT loss provides a reasonably accurate prediction of optic nerve axon loss. However, both estimates carry inherent error, so the analysis was repeated using Deming linear regression. The results of the Deming regression returned a slightly steeper slope for the relationship (1.2), but still returned a negative value for the Y-intercept (–11.3% with a 95% CI ranging from –2.0% to –21.6%) consistent with the ordinary least squares model. Thus, the Deming model indicates that the underestimate of optic nerve axon loss provided by RNFLT still is substantial before RNFLT loss is manifest, but that the underestimate is even worse at later stages of severity. For example, a value of relative RNFLT loss of 75% would be associated with essentially zero remaining axons within the anterior retrobulbar optic nerve, which is consistent with or slightly thinner than previously published estimates of the "floor effect" values for RNFLT.[12–14]

Discussion

The results of our study demonstrated that RNFLT measured in vivo by SDOCT offers a reasonably accurate representation of the total number of axons present in the anterior retrobulbar

Table 3. Pearson Correlation Coefficients (*r* Values) Resulting from Linear Regression of Optic Nerve Axon Counts versus Either RNFLT or RNFLA

	RNFLT	RNFLA
All eyes combined ($N = 38$)	0.80	0.76
EG eyes ($N = 19$)	0.78	0.75
Control eyes ($N = 19$)	0.20	0.18

This comparison is based on the subset of 19 animals for whom axial length measures were available within two weeks of sacrifice.

optic nerve (~2–3 mm behind the globe), with a Pearson correlation coefficient of 0.81 observed in this cohort. This relationship was strongest across the relatively wide range of observations from eyes with experimental glaucoma, but was considerably weaker over the relatively narrow range of observations in control eyes. An even stronger relationship was observed between relative optic nerve axon loss and relative RNFLT in glaucomatous eyes, but this is an advantage unique to unilateral experimental glaucoma, as human glaucoma and other common optic neuropathies most often are bilateral, even if asymmetric in severity. There also was a substantial degree of overlap between the distributions of values from control and glaucomatous eyes, which further underscores the challenges inherent in cross-sectional assessments of clinical diagnostic tools, such as those used to measure RNFLT.

Though the relationship between optic nerve axon number and RNFLT was correlated strongly, especially for the relative values, there was a significant offset such that approximately 10% to 15% of optic nerve axons already were lost at the point of zero relative RNFLT loss. This underestimate extends to and likely increases slightly at the more severe stages of glaucomatous loss. This might not be surprising given certain precedents published recently. For example, in two separate cohorts of monkeys with experimental glaucoma, longitudinal analysis demonstrated that there was no loss of RNFLT at the onset of optic nerve head surface topography deformation.[15,16] Yet, in an earlier histomorphometric study, albeit one without RNFLT measurements, it was determined that approximately 22% (16%–30%) of axons already were lost at a similar early stage when prelaminar tissue thickness and volume actually were increased relative to control eyes.[17] Considering that RNFLT measurement noise is approximately 6% (95% limits-of-agreement),[16] extrapolation reveals that relative axon loss will be closer to approximately 20% at the first detectable change from "normality" (or departure from baseline variation in a "suspect" with an initially normal value of RNFLT). Moreover, an additional 6% to 7% of optic nerve axons will be lost before RNFLT can be said to have changed statistically from the prior observation. Thus, clinical observations of significant RNFLT decline (i.e., worse than ~6%) from any given prior observation should raise alarm.

There are at least three possible factors to consider that might explain the discrepancy between optic nerve axon loss and RNFLT. First is a caveat that the duration between the final imaging session (RNFLT measurement) and sacrifice was 7.6 ± 5.0 days (range 0–22 days). It is possible that some progression (axon loss) occurred during this interval; however, the interval is brief relative to the average duration of post-laser follow up (>8 months). It is highly unlikely that an additional 10% to 15% loss of RNFLT occurred over this brief delay: the upper limit (97.5 percentile) of all rates of RNFLT decline ever observed over short durations in a large cohort of 59 nonhuman primates with experimental glaucoma was –0.32 μm per day,[18] which would extrapolate to less than 2.5% of RNFLT lost over 7.6 days.

It also is possible that some of the discrepancy could be attributable to gliotic changes within the RNFL,[19] or to dystrophic axonal changes, for example increasing varicosities or "beading,"[20] spherule formation,[21] axonal swelling, abortive sprouting or other form of thickening of the RNFL that would persistently offset thinning due to axon loss. Finally, it is possible that the primary site of axonal injury (e.g., an axonal transport blockade)[21–32] lies within the lamina cribrosa and that degeneration occurs faster proximal to this site than it does distally[21] (i.e., faster in the anterograde as compared to the retrograde direction), since the distances from the lamina cribrosa to the point of RNFL measurement and to the point of sampling for axon counts are approximately equal (~2 mm). Evidence of a similar phenomenon and pattern of axonal degeneration has been reported in experimental glaucoma models in rodents.[30–35]

Although a high correlation was noted between RNFLT and optic nerve axon counts over a wide range of experimental glaucoma severity in our study, this was not found across the relatively narrow range observed in control eyes. The evidence presented here finds a parallel in comparisons between RNFLT and perimetric sensitivity, whereby little correlation is observed within the normal range, but a steep and stronger relationship is noted below the lower limit of normal.[7,14] Thus, it is unlikely that RNFLT can be used as a good estimate of total axon number in normal eyes unless other constituents of the RNFL also can be measured accurately, including large[36] and small[37] blood vessels, glial tissue volume,[19] and biometric measures to account for lateral magnification of each individual eye,[38,39] which were not all measured in our study.

Axial length measures were available for 19 of the 22 pairs of eyes in our study, which were used to scale the dimension of the peripapillary circular SDOCT scan, adjusting for the lateral magnification of each individual eye. From this, the RNFL area (RNFLA) could be calculated and used to predict total optic nerve axon counts. In the group of 19 fellow control eyes, the range of RNFLA was 0.86 ± 0.076 mm^2, as has been reported previously for adult monkey eyes.[38] This result is consistent with the fact that axial length is known to exert the largest influence on lateral magnification (as compared to other anterior segment optical elements).[38,40] However, using RNFLA to predict total optic nerve axon count actually was slightly worse than using RNFLT in this subgroup of 19 animals, with Pearson correlation coefficients being slightly smaller regardless of whether all eyes were considered together or whether the 19 EG eyes and their fellow control eyes were considered separately (Table 3). This finding suggests that sources of variance other than individual differences in ocular magnification have greater influence on the relationship between RNFLT and optic nerve axon counts, and that RNFLT provides a sufficiently accurate prediction of total axon count, since use of RNFLA did not improve the predictions.

The total axon count in the 22 fellow control eyes was 1,040,225 ± 132,951 (range 812,478–1,280,474) and in the 5 pairs of bilateral control eyes it was 1,046,129 ± 160,718 (range 785,532–1,213,954), which both are consistent with previous reports for monkey optic nerves based on fractional sampling.[41–43] In contrast, estimates of total axon number derived from models based on OCT measures of RNFLT[6] are substantially (~50%) higher, which likely is due to the numerous assumptions and simplifications built into those models.

In conclusion, our study demonstrates that there is a strong linear relationship between total axon number in the optic nerve and RNFLT measured in vivo by SDOCT. However, substantial loss (~10%–15%) of optic nerve axons exists before any change in RNFLT manifests and this underestimate persists throughout a wide range of damage.

References

1. Zangwill LM, Bowd C. Retinal nerve fiber layer analysis in the diagnosis of glaucoma. *Curr Opin Ophthalmol*. 2006;17:120–131.
2. Townsend KA, Wollstein G, Schuman JS. Imaging of the retinal nerve fibre layer for glaucoma. *Br J Ophthalmol*. 2009;93:139–143.
3. Schuman JS, Pedut-Kloizman T, Pakter H, et al. Optical coherence tomography and histologic measurements of nerve fiber layer thickness in normal and glaucomatous monkey eyes. *Invest Ophthalmol Vis Sci*. 2007;48:3645–3654.
4. Weinreb RN, Kaufman PL. Glaucoma research community and FDA look to the future, II: NEI/FDA Glaucoma Clinical Trial Design and Endpoints Symposium: measures of structural change and visual function. *Invest Ophthalmol Vis Sci*. 2011;52:7842–7851.
5. Hood DC, Anderson SC, Wall M, Raza AS, Kardon RH. A test of a linear model of glaucomatous structure-function loss reveals sources of variability in retinal nerve fiber and visual field measurements. *Invest Ophthalmol Vis Sci*. 2009;50:4254–4266.
6. Harwerth RS, Wheat JL, Fredette MJ, Anderson DR. Linking structure and function in glaucoma. *Prog Retin Eye Res*. 2010;29:249–271.
7. Wollstein G, Kagemann L, Bilonick RA, et al. Retinal nerve fibre layer and visual function loss in glaucoma: the tipping point. *Br J Ophthalmol*. 2012;96:47–52.
8. Harwerth RS, Charles F. Prentice Award Lecture 2006: a neuron doctrine for glaucoma. *Optom Vis Sci*. 2008;85:436–444.
9. Reynaud J, Cull G, Wang L, et al. Automated quantification of optic nerve axons in primate glaucomatous and normal eyes–method and comparison to semi-automated manual quantification. *Invest Ophthalmol Vis Sci*. 2012;53:2951–2959.
10. Cull G, Cioffi GA, Dong J, Homer L, Wang L. Estimating normal optic nerve axon numbers in non-human primate eyes. *J Glaucoma*. 2003;12:301–306.
11. Fortune B, Cull GA, Burgoyne CF. Relative course of retinal nerve fiber layer birefringence and thickness and retinal function changes after optic nerve transection. *Invest Ophthalmol Vis Sci*. 2008;49:4444–4452.
12. Sihota R, Sony P, Gupta V, Dada T, Singh R. Diagnostic capability of optical coherence tomography in evaluating the degree of glaucomatous retinal nerve fiber damage. *Invest Ophthalmol Vis Sci*. 2006;47:2006–2010.
13. Chan CK, Miller NR. Peripapillary nerve fiber layer thickness measured by optical coherence tomography in patients with no light perception from long-standing nonglaucomatous optic neuropathies. *J Neuroophthalmol*. 2007;27:176–179.
14. Hood DC, Kardon RH. A framework for comparing structural and functional measures of glaucomatous damage. *Prog Retin Eye Res*. 2007;26:688–710.
15. Strouthidis NG, Fortune B, Yang H, Sigal IA, Burgoyne CF. Longitudinal change detected by spectral domain optical coherence tomography in the optic nerve head and peripapillary retina in experimental glaucoma. *Invest Ophthalmol Vis Sci*. 2011;52:1206–1219.
16. Fortune B, Burgoyne CF, Cull GA, Reynaud J, Wang L. Structural and functional abnormalities of retinal ganglion cells measured in vivo at the onset of optic nerve head surface change in experimental glaucoma. *Invest Ophthalmol Vis Sci*. 2012;53:3939–3950.
17. Yang H, Downs JC, Bellezza A, Thompson H, Burgoyne CF. 3-D histomorphometry of the normal and early glaucomatous monkey optic nerve head: prelaminar neural tissues and cupping. *Invest Ophthalmol Vis Sci*. 2007;48:5068–5084.
18. Gardiner SK, Fortune B, Wang L, Downs JC, Burgoyne CF. Intraocular pressure magnitude and variability as predictors of rates of structural change in non-human primate experimental glaucoma. *Exp Eye Res*. 2012;103:1–8.
19. Wang L, Cioffi GA, Cull G, Dong J, Fortune B. Immunohistologic evidence for retinal glial cell changes in human glaucoma. *Invest Ophthalmol Vis Sci*. 2002;43:1088–1094.
20. Wang L, Dong J, Cull G, Fortune B, Cioffi GA. Varicosities of intraretinal ganglion cell axons in human and nonhuman primates. *Invest Ophthalmol Vis Sci*. 2003;44:2–9.
21. Coleman M. Axon degeneration mechanisms: commonality amid diversity. *Nat Rev Neurosci*. 2005;6:889–898.
22. Anderson DR, Hendrickson A. Effect of intraocular pressure on rapid axoplasmic transport in monkey optic nerve. *Invest Ophthalmol*. 1974;13:771–783.
23. Quigley H, Anderson DR. The dynamics and location of axonal transport blockade by acute intraocular pressure elevation in primate optic nerve. *Invest Ophthalmol*. 1976;15:606–616.
24. Minckler DS, Bunt AH, Klock IB. Radioautographic and cytochemical ultrastructural studies of axoplasmic transport in the monkey optic nerve head. *Invest Ophthalmol Vis Sci*. 1978;17:33–50.
25. Quigley HA, Guy J, Anderson DR. Blockade of rapid axonal transport. Effect of intraocular pressure elevation in primate optic nerve. *Arch Ophthalmol*. 1979;97:525–531.
26. Quigley HA, Addicks EM. Chronic experimental glaucoma in primates. II. Effect of extended intraocular pressure elevation on optic nerve head and axonal transport. *Invest Ophthalmol Vis Sci*. 1980;19:137–152.
27. Martin KR, Quigley HA, Valenta D, Kielczewski J, Pease ME. Optic nerve dynein motor protein distribution changes with intraocular pressure elevation in a rat model of glaucoma. *Exp Eye Res*. 2006;83:255–262.
28. Balaratnasingam C, Morgan WH, Bass L, Matich G, Cringle SJ, Yu DY. Axonal transport and cytoskeletal changes in the laminar regions after elevated intraocular pressure. *Invest Ophthalmol Vis Sci*. 2007;48:3632–3644.
29. Balaratnasingam C, Morgan WH, Bass L, Cringle SJ, Yu DY. Time-dependent effects of elevated intraocular pressure on optic nerve head axonal transport and cytoskeleton proteins. *Invest Ophthalmol Vis Sci*. 2008;49:986–999.
30. Buckingham BP, Inman DM, Lambert W, et al. Progressive ganglion cell degeneration precedes neuronal loss in a mouse model of glaucoma. *J Neurosci*. 2008;28:2735–2744.
31. Salinas-Navarro M, Alarcon-Martinez L, Valiente-Soriano FJ, et al. Ocular hypertension impairs optic nerve axonal transport leading to progressive retinal ganglion cell degeneration. *Exp Eye Res*. 2010;90:168–183.
32. Crish SD, Sappington RM, Inman DM, Horner PJ, Calkins DJ. Distal axonopathy with structural persistence in glaucomatous neurodegeneration. *Proc Natl Acad Sci U S A*. 2010;107:5196–5201.
33. Howell GR, Libby RT, Jakobs TC, et al. Axons of retinal ganglion cells are insulted in the optic nerve early in DBA/2J glaucoma. *J Cell Biol*. 2007;179:1523–1537.
34. Soto I, Oglesby E, Buckingham BP, et al. Retinal ganglion cells downregulate gene expression and lose their axons within the optic nerve head in a mouse glaucoma model. *J Neurosci*. 2008;28:548–561.
35. Soto I, Pease ME, Son JL, Shi X, Quigley HA, Marsh-Armstrong N. Retinal ganglion cell loss in a rat ocular hypertension model is sectorial and involves early optic nerve axon loss. *Invest Ophthalmol Vis Sci*. 2011;52:434–441.

36. Hood DC, Fortune B, Arthur SN, et al. Blood vessel contributions to retinal nerve fiber layer thickness profiles measured with optical coherence tomography. *J Glaucoma*. 2008;17:519–528.
37. Scoles D, Gray DC, Hunter JJ, et al. In-vivo imaging of retinal nerve fiber layer vasculature: imaging histology comparison. *BMC Ophthalmol*. 2009;9:9.
38. Patel NB, Luo X, Wheat JL, Harwerth RS. Retinal nerve fiber layer assessment: area versus thickness measurements from elliptical scans centered on the optic nerve. *Invest Ophthalmol Vis Sci*. 2011;52:2477–2489.
39. Patel NB, Wheat JL, Rodriguez A, Tran V, Harwerth RS. Agreement between retinal nerve fiber layer measures from Spectralis and Cirrus spectral domain OCT. *Optom Vis Sci*. 2012;89:E652–E666.
40. Patel NB, Garcia B, Harwerth RS. Influence of anterior segment power on the scan path and RNFL thickness using SD OCT. *Invest Ophthalmol Vis Sci*. 2012;53:5788–5798.
41. Sanchez RM, Dunkelberger GR, Quigley HA. The number and diameter distribution of axons in the monkey optic nerve. *Invest Ophthalmol Vis Sci*. 1986;27:1342–1350.
42. Yucel YH, Kalichman MW, Mizisin AP, Powell HC, Weinreb RN. Histomorphometric analysis of optic nerve changes in experimental glaucoma. *J Glaucoma*. 1999;8:38–45.
43. Kerrison JB, Buchanan K, Rosenberg ML, et al. Quantification of optic nerve axon loss associated with a relative afferent pupillary defect in the monkey. *Arch Ophthalmol*. 2001;119:1333–1341.